Electronic and vibrational spectra of two-dimensional quasicrystals

T. Odagaki* and D. Nguyen
Department of Physics, Brandeis University, Waltham, Massachusetts 02254
(Received 8 August 1985)

The tight-binding electronic structure of two-dimensional quasicrystals is studied numerically for three patterns of Penrose tiling with up to 426 vertices. According to the range of interactions, three different models are considered. For the simplest model, two different interactions are assigned to long and short edges of the Penrose tile. Energy spectra show several significant gaps whose width and position depend on the relative strength of the interactions. The cumulative density of states is linear in energy at the band edge, indicating the existence of the Van Hove singularities. The energy spectra for other models show similar band gaps and singularities, though the density of states is asymmetric. Participation ratios are examined. When the relative strength of interactions becomes small, significant numbers of states become localized. Lattice vibration perpendicular to the plane is studied in the harmonic approximation for the simplest model. The vibrational spectra show gaps and singularities similar to the electronic spectra.

I. INTRODUCTION

Recently, quasicrystals, nonperiodic lattices with a long-range bond-orientational order, have attracted wide interest as a new class of ordered condensed state. Rapidly quenched alloys of Al with Mn, Fe, or Cr are conjectured to be such systems in three dimensions with icosahedral point-group symmetry,[1-5] which is inconsistent with long-range translational symmetry. The stability of this structure has also been studied on the basis of the Landau theory of phase transitions.[6] Bak[7] argued that the structure could be classified as an incommensurate structure with one length scale and is not a fundamentally new state. Since the quasicrystal structure is situated between regular crystals and completely disordered systems, the fundamental physical properties of quasicrystals are expected to have very interesting features. In this paper, we study the electronic and vibrational properties of two-dimensional quasicrystals.

An example of two-dimensional quasicrystals is the vertices of the Penrose tiling.[8-10] In the Penrose tiling, two tiles, the so-called kite and dart, fill the two-dimensional space only nonperiodically. Each tile consists of two long and short edges, the ratio of the length of the long and short edges being $\tau \equiv (\sqrt{5}+1)/2 = 1.61803\ldots$, the golden ratio. There are an infinite number of Penrose tilings, each of which is made up of kites and darts in the ratio τ:1. The tiling has various amazing properties.[9] For example, any finite-size region in any tiling is contained somewhere inside every tiling (Penrose's local isomorphism theorem), and a circular region of diameter d is never more than $2d$ away from an exactly identical region (Conway's town theorem). Most of the tiles belong to local-pentagonally symmetric regions. Among the infinite number of tilings, two tilings we will investigate are very attractive, since they have a fivefold rotational symmetry axis. The existence of a fivefold rotational symmetry axis indicates an absence of translational symmetry.

In this paper, we investigate numerically the properties of the electronic states of a tight-binding Hamiltonian and vibrational states in the harmonic approximation in finite Penrose tilings. We study three different tilings, with up to 426 vertices. The essential features of the conclusions drawn in the following should be independent of the choice of tiling. We obtain the spectra of the tight-binding Hamiltonian and the lattice vibration by computer simulation, assigning different interactions to different bonds. Among interesting questions to be asked are: (1) Is there any band gap, like in a binary-bond system in regular crystals? (2) Does the Van Hove singularity appear in the spectra? (Note that the existence of the singularities in periodic crystals was first proved on the basis of the topology of the energy band in the reciprocal-lattice space.[11]) (3) Are the eigenfunctions extended?

Similar spectra for one-dimensional quasicrystals has been studied recently.[12] The one-dimensional spectra show a lot of band gaps and Van Hove singularities as well.

In Sec. II, we present model systems to be studied. Assuming different interactions between vertices of the Penrose tilings, we examine three different models. We also discuss the distribution of the coordination number in Sec. II. We show numerical results for the density of states and the participation ratios in Secs. III and IV. Concluding remarks are given in Sec. V. In Sec. V, we also include the energy spectrum of a one-dimensional quasicrystal, the Fibonacci chain, for comparison.

II. MODEL AND DEFINITIONS

We consider the tightbinding Hamiltonian

$$H = \sum_{i \neq j} |i\rangle t_{ij} \langle j| \ , \tag{2.1}$$

where $\{|i\rangle\}$ is assumed to be an orthonormal set and the state $|i\rangle$ is associated with the ith vertex of a Penrose tiling. Different specifications of the range of the transfer integral lead to different models such as

Model I: $t_{ij}\neq 0$ when sites i and j are the end points of an edge of tiles, and $t_{ij}=0$ otherwise. According to whether it corresponds to a long or short edge, t_{ij} takes the value of either $-t_L$ or $-t_S$.

Model II: $t_{ij}\neq 0$ as in model I and also when site i and j are the end points of the symmetric diagonal of a tile, and $t_{ij}=0$ otherwise. Note that the length of the symmetric diagonal of a kite is the same as that of the long edge, and the length of the symmetric diagonal of a dart is the same as that of the short edge.

Model III: $t_{ij}\neq 0$ when the distance between sites i and j is shorter or equal to the length of the long edge of tiles.

For model I, $t_S(>0)$ is chosen to be a scaling factor and t_L is continuously changed. For models II and III,

$$t_{ij}=-t_S\exp[-(r_{ij}-r_S)/r_S]$$

is used where r_{ij} and r_S are the distance between sites i and j and the short edge of the tiles, respectively, and t_S (>0) is the scale of energy.

For the lattice vibration, we consider a set of equations

$$m\ddot{u}_i=-\sum_{j\neq i}k_{ij}(u_j-u_i)\ , \tag{2.2}$$

where u_i is the displacement of mass, m, placed at vertex i of a Penrose tiling perpendicular to the plane and k_{ij} is the force constant between vertices i and j. Assuming $u_i=a_ie^{-i\omega t}$, Eq. (2.2) reduces to

$$m\omega^2a_i=\sum_{j\neq i}k_{ij}(a_j-a_i)\ . \tag{2.3}$$

We consider Model I for the lattice vibration with $k_{ij}=k_L$ or k_S.

Three Penrose tilings, T1 with 426 vertices, T2 with 381 vertices, and T3 with 391 vertices are studied in the following (these are named the "Star," the "Sun," and the "Cartwheel," respectively, in Ref. 9). T1 and T2 have a fivefold symmetry axis and they can be interchanged by "inflation" or "deflation" transformations.[9] T3 has tenfold symmetry except for the central "cartwheel" and ten radial spokes.[9] Any vertex of Penrose tilings must be one of seven types:[13] V1 (consists of five kites), V2 (five darts), V3 (two kites and one dart), V4 (two kites and two darts), V5 (three kites and two darts), V6 (four kites and one dart), and V7 (two kites and three darts). Figure 1 shows these seven types together with the nonzero interactions in model II. In model I, V1, V2, V5, V6, and V7 have five neighbors, and V3 and V4 have three and four neighbors, respectively. Table I shows the distribution of the seven types of vertices for the tilings we studied, where vertices in the outermost shell are not counted.

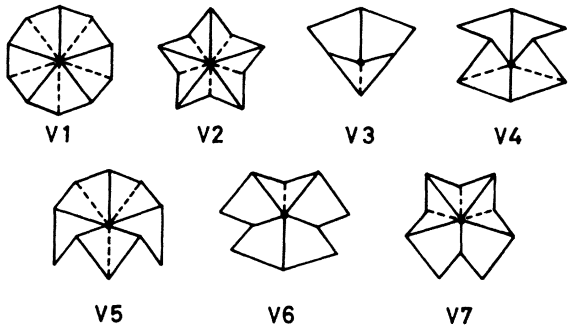

FIG. 1. Two unit tiles (kite and dart) make seven different vertices in the Penrose tiling. For example, the V1 vertex is made of five kites and the V2 vertex is made of five darts. In model I, interaction is introduced along the edge of tiles. Dashed lines are the interactions included in model II for the center vertex.

In the following sections, we diagonalize the Hamiltonian matrix or the dynamical matrix and obtain eigenvalues and eigenfunctions. We calculate the density of states $D(\epsilon)$ and the cumulative density of states $N(\epsilon)$ which are defined, respectively, by

$$D(\epsilon)=\frac{1}{N}\sum_{\mu}\delta(\epsilon-\epsilon_\mu)\ , \tag{2.4}$$

where N is the total number of vertices and $\{\epsilon_\mu\}$ are the eigenvalues, and by

TABLE I. Configuration of vertices in the Penrose tilings. The average coordination number is very close to 4 for these patterns.

Type	Coordination number in model I	=	Number of long edges	+	short edges	T1 total 366 (%)	T2 total 301 (%)	T3 total 311 (%)
V1	5	=	5	+	0	21 (5.74)	25 (8.31)	23 (7.40)
V2	5	=	5	+	0	10 (2.73)	6 (1.99)	13 (4.18)
V3	3	=	1	+	2	145 (39.62)	115 (38.21)	125 (40.19)
V4	4	=	1	+	3	90 (24.59)	70 (23.26)	65 (20.90)
V5	5	=	3	+	2	55 (15.03)	40 (13.29)	45 (14.47)
V6	5	=	3	+	2	25 (6.83)	25 (8.31)	25 (8.04)
V7	5	=	4	+	1	20 (5.46)	20 (6.64)	15 (4.82)

$$N(\epsilon)=\int_{-\infty}^{\epsilon} D(\epsilon')d\epsilon' . \tag{2.5}$$

We also calculate the participation ratio,[14] P_μ, for each eigenstate. The participation ratio is defined by

$$P_\mu=\frac{\sum_i |a_i^\mu|^2}{N\sum_i |a_i^\mu|^4} , \tag{2.6}$$

where the eigenfunction $|\mu\rangle$ of the tight-binding system is expanded as

$$|\mu\rangle=\sum_i a_i^\mu |i\rangle . \tag{2.7}$$

For the lattice vibration, a_i^μ represents the displacement of vertex i in the μth eigenmode. The participation ratio takes the value $1/N$ when the eigenfunction is localized in a single site, and it is unity when the eigenfunction is extended uniformly over the system.

III. ENERGY SPECTRA FOR THE TIGHT-BINDING HAMILTONIAN

A. Model I

Changing the relative strength of the transfer energy t_L/t_S continuously, we obtained energy eigenvalues. Figure 2 shows the energy eigenvalues in the t_L/t_S versus energy E/t_S plane for (a) T1, (b) T2, and (c) T3. A lot of spectral gaps can be seen in Fig. 2, some of which are due to the finiteness of the system size. Wider spectral gaps do not seem to depend severely on the system size, indicating they will persist in an infinite system. (See Sec. IV for comparison of different system sizes.) In the limit $t_L/t_S=0$, the system has some isolated clusters as well as infinitely connected channels. A novel point to see is that even when $t_L=t_S$, i.e., all the interactions along long edges and short edges are common, spectral gaps appear around $E=0$. The geometrical structure must be responsible for these gaps.

In Figs. 3–5 we show the histograms of the density of states and the cumulative density of states for three different values, $t_L/t_S=1.0$, 0.6, and 0.0. The density of states for $t_L/t_S=1$ looks very similar to that of the square lattice except for the spectral gaps around $E=0$. The cumulative density of states is linear in E at the band edge, suggesting that Van Hove singularities exist there. The envelope of the density of states also suggests the divergence of the density of states at $E=0$, which is another Van Hove singularity in two dimensions.

In these figures, we also plotted the participation ratios for all eigenstates. Although we do not see any clear mobility edges nor any threshold for t_L/t_S, some of the eigenstates look localized when t_L/t_S is small.

B. Models II and III

Figures 6 and 7 show the density of states together with the participation ratios and the cumulative density of states for model II and III, respectively. In model II,

$$t_L=t_S\exp[-(r_L-r_S)/r_S]$$

is assumed, where r_L is the length of a long edge of the tile. The density of states is asymmetric and very similar to that of the triangular lattice. Both spectra show clear Van Hove singularities at the band edges and a number of small gaps which may persist in the infinite system.

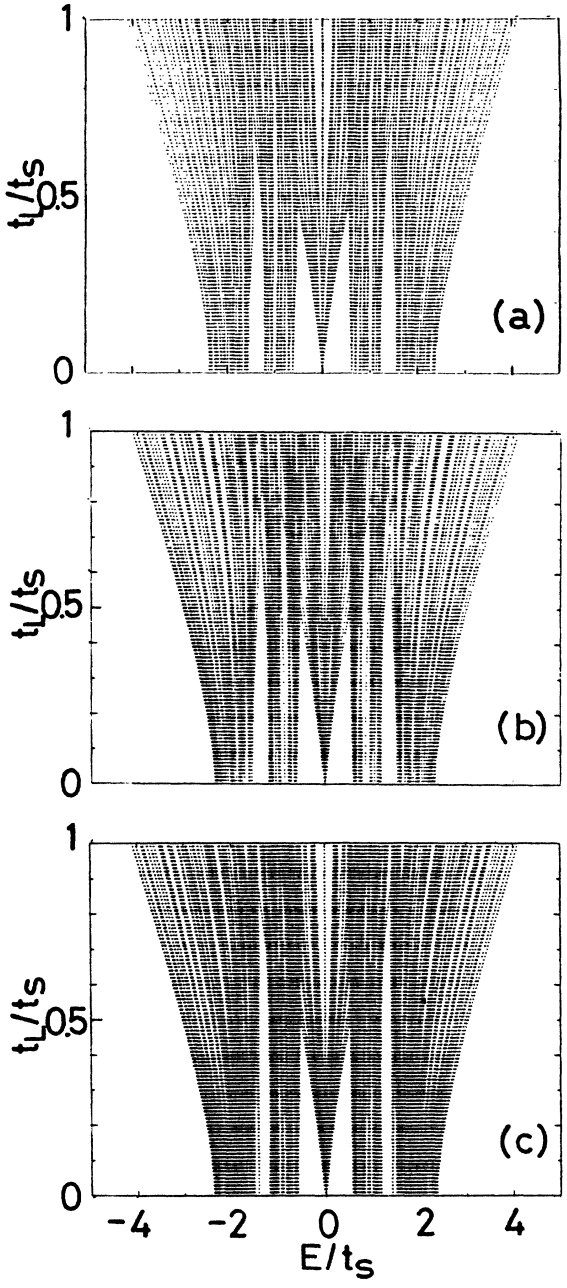

FIG. 2. Spectral gaps in the tight-binding electronic structure for the Penrose tiling model of two-dimensional quasicrystals, model I: (a) T1 (426 sites), (b) T2 (381 sites), and (c) T3 (391 sites). A dot corresponds to an eigenenergy for a particular relative strength t_L/t_S of the interactions. Smaller gaps may disappear as the system size is increased, while larger gaps will persist in the infinite system.

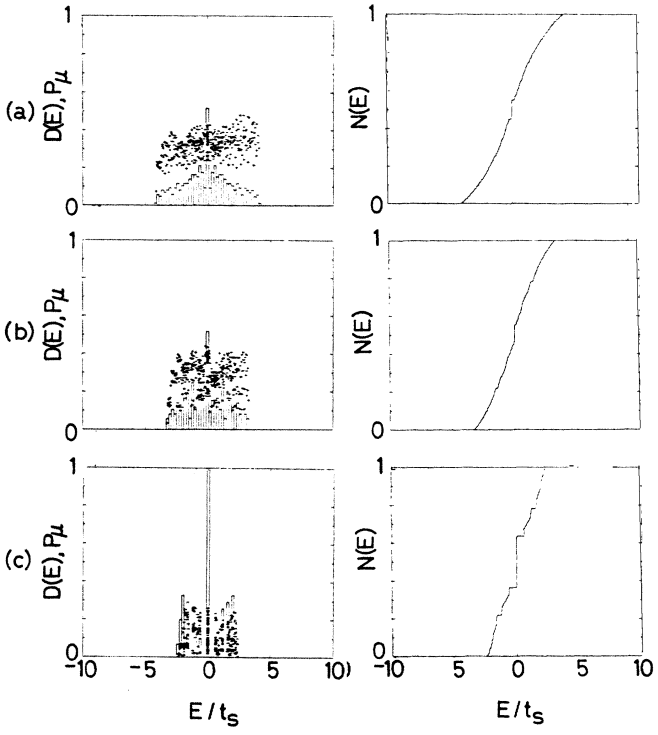

FIG. 3. Density of states $D(E)$ and the cumulative density of states $N(E)$ for the tight-binding system in the finite T1 pattern, model I: (a) $t_L/t_S=1$, (b) $t_L/t_S=0.6$, (c) $t_L/t_S=0$. + signs denote the participation ratio of each eigenstate.

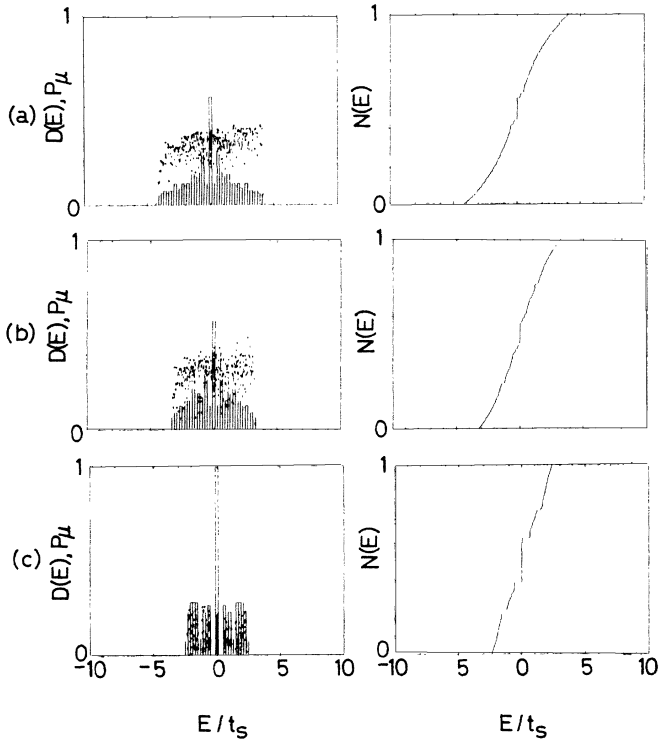

FIG. 5. Similar to Fig. 3 for T3.

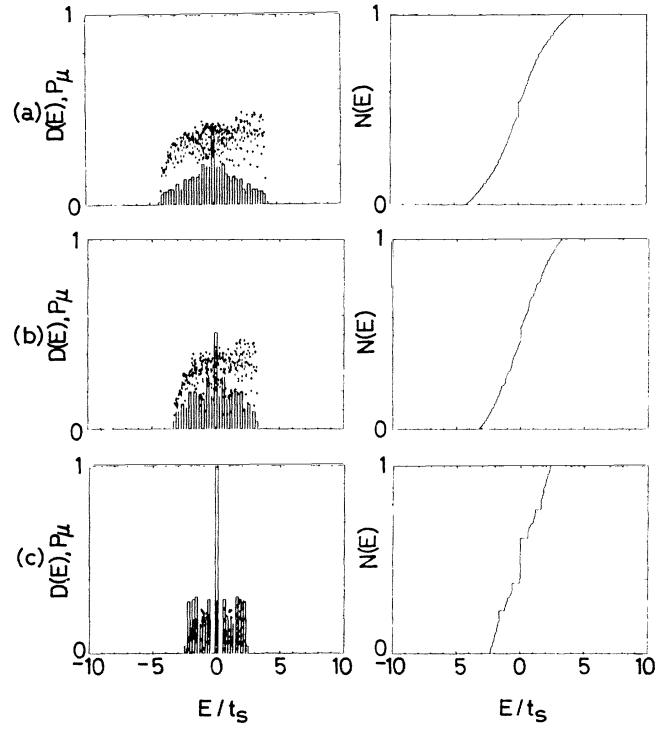

FIG. 4. Similar to Fig. 3 for T2.

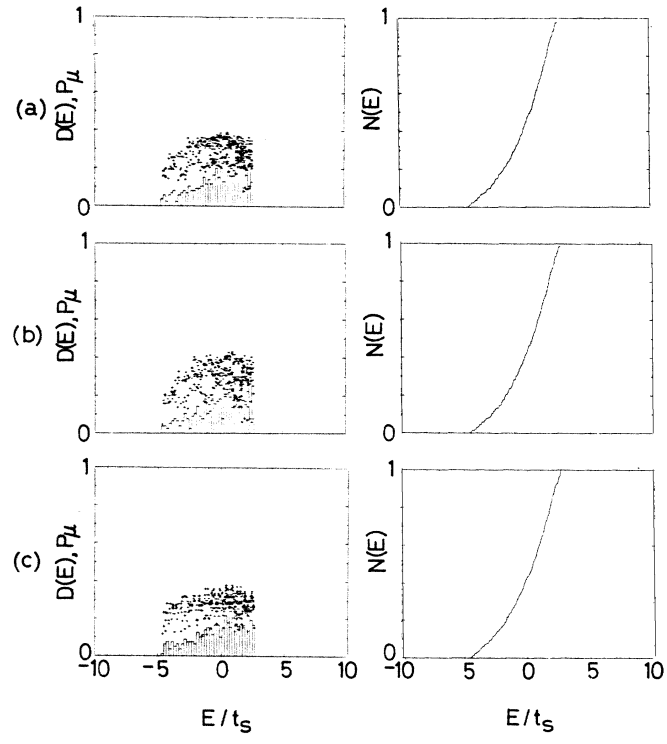

FIG. 6. Density of states $D(E)$ and the cumulative density of states $N(E)$ for the tight-binding system in the finite Penrose tiling, model II: (a) T1, (b) T2, (c) T3.

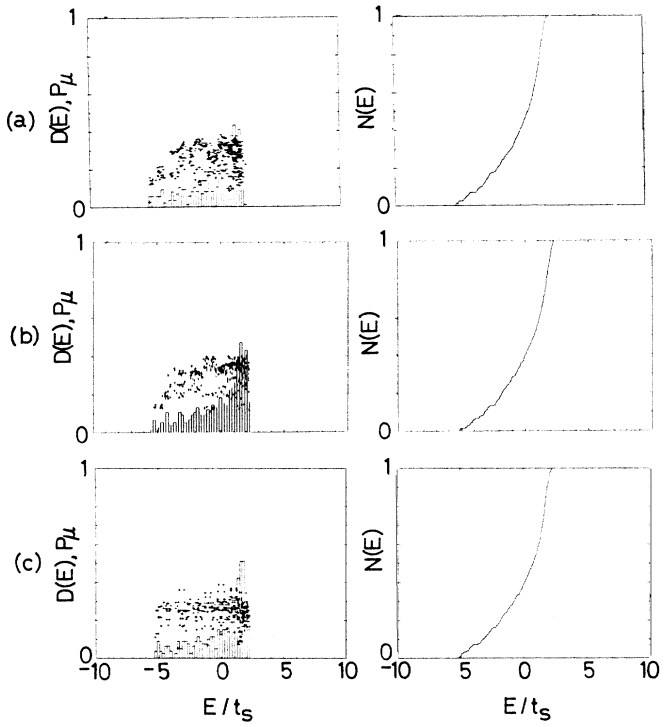

FIG. 7. Similar to Fig. 6 for model III.

IV. FREQUENCY SPECTRA FOR THE LATTICE VIBRATION

In Fig. 8, we show the eigenfrequencies as functions of the relative strength k_L/k_S of the spring constants for three different sizes of the T3 pattern. As the system size is increased, some of the gaps become smaller, suggesting the gaps are due to the finiteness of the system. However, there are several gaps which become clearer as the system size is increased. These gaps will persist in the infinite system. Similar gaps have been observed in the spectra of the T1 and T2 patterns.

Figure 9 shows the density of states $D(\omega^2)$ together with the participation ratios and the cumulative density of states for the relative strength of the force constant $k_L/k_S=1.0$, 0.4, 0.0. We see clear Van Hove singularities at the band edge except for the lower band edge when $k_L/k_S=0$, since the cumulative density of states is linear in ω^2 there. The lower band edge for $k_L/k_S=0$ also seems to be linear in ω^2 if the degenerate modes due to isolated clusters are removed. Although another type of the Van Hove singularity in two-dimensions cannot be seen clearly in these figures, the density of states for $k_L/k_S=1$ and 0.4 have a rather sharp peak in $D(\omega^2)$, showing that the singularity may exist.

Participation ratios again indicate some of the eigenmodes are localized when k_L/k_S is small. The number of localized modes becomes significant when $k_L/k_S \lesssim 0.4$.

V. CONCLUDING REMARKS

We have obtained numerically the energy and frequency spectra of a tight-binding system and of the lattice vibration in two-dimensional quasicrystals. The density of states for different patterns of Penrose tiling appear to be very similar. This is probably due to the local isomorphism of the Penrose tiling. The spectra show several gaps even when the interactions are uniform. Near the band edge Van Hove singularities seem to exist. Namely, the electronic spectrum near the lower band edge has the same singularity as the free-electron spectrum. These properties of the spectra should be carried over to the infinite system. We studied the nature of the eigenfunctions with the participation ratio. Our data for model I suggest that localized states exist when the relative strength of the interactions is small, and the number of localized states

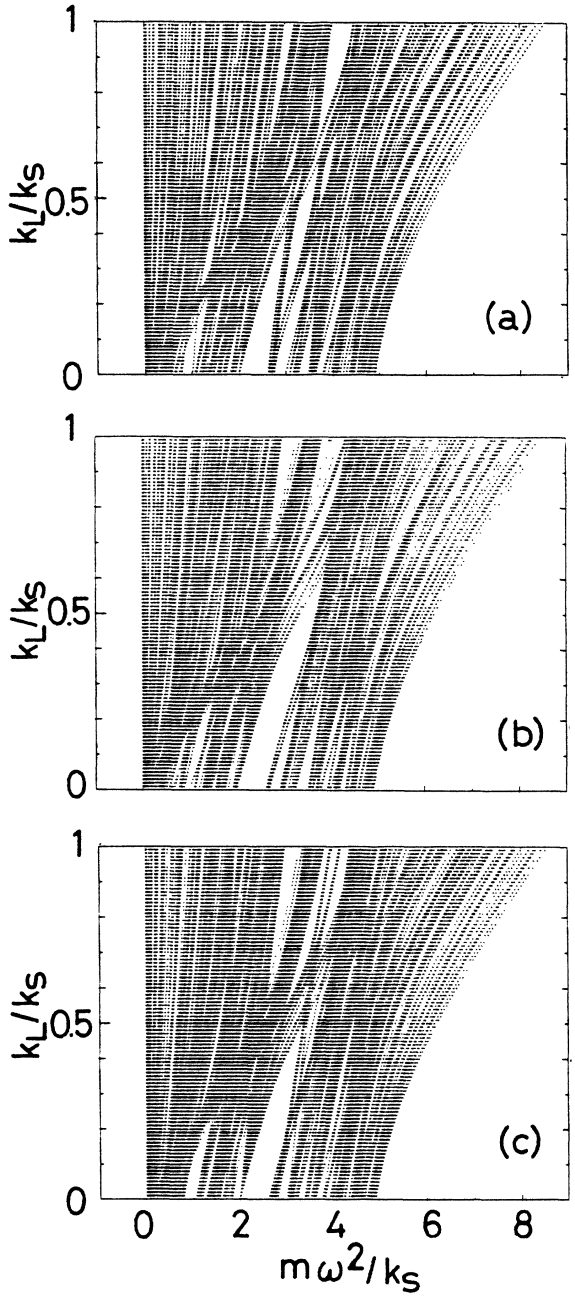

FIG. 8. System size dependence of the spectral gaps in the vibrational spectra for T3, model I. (a) 251 sites, (b) 311 sites, (c) 391 sites.

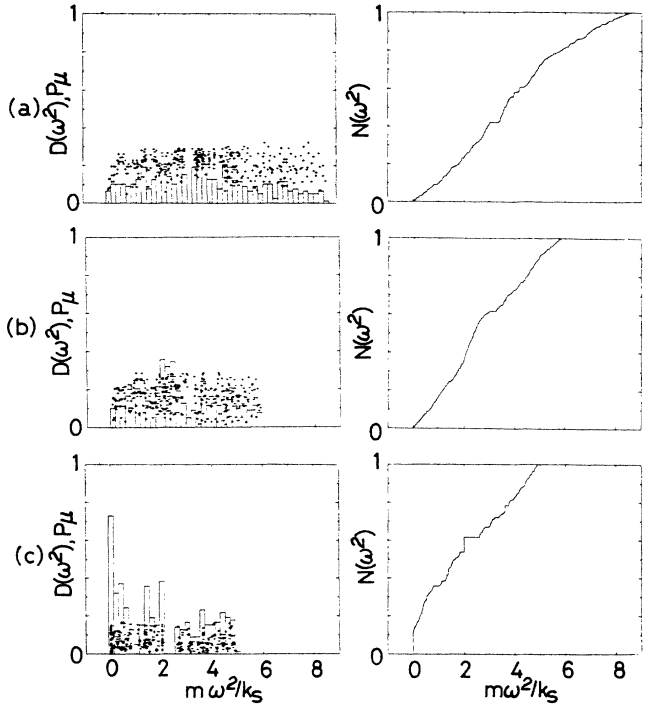

FIG. 9. Density of states $D(\omega^2)$ and the cumulative density of states $N(\omega^2)$ for the lattice vibration of the finite T3 pattern with 391 sites: (a) $k_L/k_S=1$, (b) $k_L/k_S=0.4$, (c) $k_L/k_S=0$. + signs denote the participation ratio of each eigenmode.

becomes significant when the ratio of the interactions (t_L/t_S or k_L/k_S) is below 0.4. The situation for t_L (or k_L)=0 is very interesting, since the system now consists of only the short edges of Penrose tiles. The short edges form infinite paths as well as isolated decagons. The eigenvalues for an isolated decagon are given by $E/t_S=2, \pm\tau, \pm(\tau-1), -2$, where the states $E/t_S=\pm\tau$ and $\pm(\tau-1)$ are doubly degenerate (τ is the golden ratio). The present results show that some eigenstates are localized, while some are extended within the length scale observed. The localization of eigenstates is caused probably by the irregularity of the infinite channel, the same reason that the quantum percolation threshold is different from the classical one.[15] Spectral gaps around the central peak have been observed in the quantum percolation model, too.[16]

The density of states of a tight-binding system is symmetric for model I and asymmetric for models II and III with respect to $E=0$. This is because the number of vertices along any path which starts a vertex and returns to the vertex passing vertices connected by a nonzero transfer energy is always even for model I and can be odd for models II and III.

Recently, the spectra of one-dimensional quasicrystals have been studied extensively.[12,17–20] We present here some results for the tight-binding system in the Fibonacci chain, where the chain consists of two basic units A and B, in the order of

$$ABAABABAABAAB\ldots .$$

We assign interaction $-t_A$ to A and $-t_B$ to

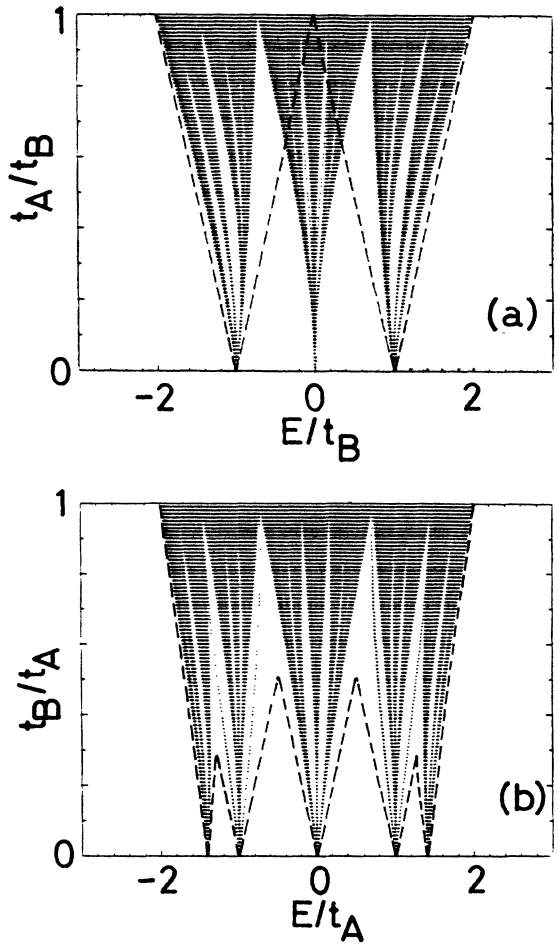

FIG. 10. Spectral gaps in the tight-binding electronic structure for the Fibonacci chain with 988 sites, a one-dimensional quasicrystal. The dashed curves represent (a) the band edges for the AB regular chain and (b) the common band edges for AB and AAB regular chains.

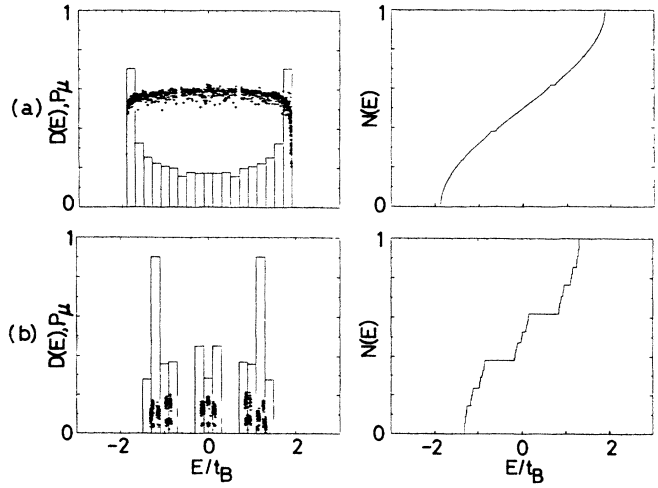

FIG. 11. Density of states $D(E)$ and the cumulative density of states $N(E)$ for the tight-binding system in the Fibonacci chain: (a) $t_A/t_B=0.9$, (b) $t_A/t_B=0.4$. + signs denote the participation ratio of each eigenstate.

B (t_A, $t_B \geq 0$). Changing t_A/t_B and t_B/t_A between 0 and 1, we obtained the energy spectra for the Fibonacci chain with 988 sites. Figure 10 shows the structure of the spectral gaps. Figure 10(b) resembles very closely Fig. 9(b) of Ref. 12. Note that when $t_A/t_B=0$ the system consists of isolated sites and two-site clusters and when $t_B/t_A=0$, the system consists of two- and three-site clusters. Also note that when $t_A/t_B=1$ the chain is regular. In Fig. 11 the density of states with the participation ratios and the cumulative density of states are plotted for $t_A/t_B=0.9$ and 0.4. The cumulative density of states shows self-similarity as observed before.[12] Within the length scale studied there seems to be a mobility edge near the upper band edge, and most of the states become localized when $t_A/t_B<0.4$. Further studies are needed to conclude if these properties exist in the infinite chain.

ACKNOWLEDGMENTS

This work was supported in part by a grant from Research Corporation. We would like to thank Professor J. L. Birman and J. P. Lu of City College of New York for helpful discussions.

---

*Also at GTE Laboratories, Waltham, Massachusetts 02154.

[1]D. S. Shechtman, I. Blech, D. Gratias, and J. W. Chan, Phys. Rev. Lett. **53**, 1951 (1984).

[2]D. Levine and P. J. Steinhardt, Phys. Rev. Lett. **53**, 2477 (1984).

[3]P. A. Bancel, P. A. Heiney, P. W. Stephens, A. I. Goldman, and P. M. Horn, Phys. Rev. Lett. **54**, 2432 (1985).

[4]P. A. Kalugin, A. Yu. Kitaev, and L. S. Levitov, Pis'ma Zh. Eksp. Teor. Fiz. **41**, 119 (1985) [JETP Lett. **41**, 145 (1985)].

[5]V. Elser, Phys. Rev. B **32**, 4892 (1985).

[6]N. D. Mermin and S. M. Troian, Phys. Rev. Lett. **54**, 1524 (1985).

[7]P. Bak, Phys. Rev. Lett. **54**, 1517 (1985).

[8]R. Penrose, Bull. Inst. Math. Appl. **10**, 266 (1974).

[9]M. Gardner, Sci. Am. **236**, 110 (1977).

[10]A. L. Mackay, Physica A **114**, 609 (1982).

[11]L. Van Hove, Phys. Rev. **89**, 1189 (1953).

[12]J. P. Lu, T. Odagaki and J. L. Birman (unpublished).

[13]Penrose tilings can be generated with two rhombi (see Refs. 9 and 10). This method introduces an extra point in each kite. In this Penrose tiling there are seven types of vertices again; the vertices corresponding to V1 and V2 are locally indistinguishable, but the extra point in each kite makes a vertex different from others.

[14]P. Dean, Proc. Phys. Soc. London **73**, 413 (1959).

[15]T. Odagaki and K. C. Chang, Phys. Rev. B **30**, 1612 (1984).

[16]T. Odagaki, N. Ogita, and H. Matsuda, J. Phys. C **13**, 189 (1980); T. Odagaki and F. Yonezawa, J. Phys. Soc. Jpn. **47**, 379 (1979).

[17]M. Kohmoto, L. P. Kadanoff, and C. Tang, Phys. Rev. Lett. **50**, 1870 (1983).

[18]S. Ostlund, R. Pandit, D. Rand, H. J. Schellnhuber, and E. D. Siggia, Phys. Rev. Lett. **50**, 1873 (1983).

[19]S. Ostlund and R. Pandit, Phys. Rev. B **29**, 1394 (1984).

[20]T. Nagatani, Phys. Rev. B **32**, 2049 (1985).